

Dynamic Properties of Rain Attenuation in Athens, Greece: Slant Path Rain Attenuation Synthesizer and Dynamic Diversity Gain

Charilaos Kourogiorgas¹, Athanasios D. Panagopoulos^{1, *},
Spiros N. Livieratos², and George E. Chatzarakis²

Abstract—In this paper, the dynamics of rain attenuation are examined, and dynamic diversity gain is evaluated for a pico-scale site diversity system. Since modern satellite communication systems operate at frequencies above 10 GHz, their efficient design requires the adoption of Propagation Impairment Mitigation techniques and so rain attenuation time series synthesizers. For rain attenuation, which is the most dominant fading mechanism, the dynamic stochastic model, proposed by Maseng-Bakken, based on the lognormal distribution is the most widely accepted and used. In this latter model, the dynamic parameter is required for the generation of slant path rain attenuation time series. In this paper, firstly, a simple expression is proposed for the calculation of the dynamic parameter in terms of the mean wind speed, elevation angle of the link, and dynamic parameter of rainfall rate. The new theoretical expression is tested with simulated data with very encouraging results. This expression is then used into a unified rain attenuation synthesizer with inputs from the rainfall rate statistics and the satellite slant path characteristics. Finally, the dynamic diversity gain is calculated for pico-scale site diversity systems for various link characteristics.

1. INTRODUCTION

The migration of the operating frequencies at Ka-band and above is due to the congestion of conventional frequency bands and the higher available bandwidth. At these high frequency bands, the atmospheric phenomena affect signal propagation. Rain fading is the worst propagation factor that deteriorates the system's performance. For compensating the several dB of atmospheric attenuation without significantly increasing system margins, Propagation Impairment Mitigation Techniques have been identified [1], and most of them are already employed in DVB-S2 standardized satellite systems [2]. Such techniques include adaptive techniques which depend on the dynamics of atmospheric attenuation.

Therefore, for the evaluation of the system's performance simultaneously adopting PIMTs, time series synthesizers of rain attenuation are needed. One of the most widely used rain attenuation time series generator is the dynamic stochastic model presented firstly in [3]. In this model, rain attenuation is modeled as a stochastic process and described with a first-order stochastic differential equation. Among the parameters of this model, the dynamic parameter is defined which is related to the autocorrelation of rain attenuation and so the rain attenuation dynamics. This parameter depends on the geometrical, electrical link characteristics and the properties of rainfall medium, as this has been pointed out also in the related references [3–6]. In [7, 8], expressions for the calculation of dynamic parameter for terrestrial links based on experimental data have been proposed recently.

Moreover, a very effective but cost-inefficient PIMT is site diversity [1]. In site diversity systems two or more base stations are communicating with the same satellite. Therefore, exploiting the spatial variations of rainfall medium, the probability of the simultaneous exceedance of rain attenuation becomes

Received 27 November 2014, Accepted 30 January 2015, Scheduled 5 February 2015

* Corresponding author: Athanasios D. Panagopoulos (thpanag@ece.ntua.gr).

¹ School of Electrical and Computer Engineering, National Technical University of Athens, Athens, Greece. ² Departments of Electrical and Electronic Engineering Educators, School of Pedagogical and Technological Education, Athens, Greece.

lower than the exceedance of rain attenuation on a single link. In [9], the metric of dynamic diversity gain is introduced which gives the diversity gain on temporal domain. In site diversity systems, the larger the separation distance is between the two ground stations, the lower the outage probability is. However, there are special categories of site diversity systems such as the short-scale, micro-scale or pico-scale site diversity systems [9, 10], which have not been studied in depth. Pico-scale diversity can be applied to the sports events broadcasting when the ground stations are close to each other around the stadium.

In this paper, firstly, a simple expression is derived and proposed for the calculation of the dynamic parameter for the generation of slant path rain attenuation time series. The expression is obtained using synthesized rain attenuation time series applying the Synthetic Storm Technique [11] (SST) to rain rate measurements obtained inside the campus of National Technical University of Athens (NTUA) [6]. The SST is used only as a substitute of beacon measurements, in order to proceed to the parametrization of the dynamic parameter of rain attenuation. Then using the proposed expression for the dynamic parameter, a unified synthesizer is proposed using Stochastic Differential Equations (SDEs) [4, 12, 13] with inputs from the rainfall rate statistics and the satellite link geometrical and electrical characteristics. The second part of the manuscript is devoted to the investigation of the dynamic properties of rain attenuation in pico-scale site diversity systems. The dynamic diversity gain is explained and evaluated using synthesized rain attenuation time series for two stations separated 387 m distance. In the numerical results section, the proposed expression is given as a function of the wind speed and elevation angle, and then, it is tested with very good results. Finally, the first-order statistics of the dynamic diversity gain of the pico-scale site diversity system are presented for various cases.

2. RAIN ATTENUATION DYNAMICS

In this section, firstly the rain rate dataset is briefly explained, and then the rain attenuation dynamics assumed in this paper are given.

As firstly presented in [6], rain rate time series were measured in two sites inside the NTUA campus with a 387 m separation distance. Two tipping buckets have been placed at the campus of National Technical University of Athens with a resolution of 0.2 mm per tip. In this paper, the measurements for 2 consecutive years have been employed. From the measured rainfall amount per tip the rain rate has been calculated according to the methodology given in [14] and also used in [15]. In Fig. 1, the CCDF of rain rate for the 2-year period is given for both sites.

Using the SST, rain attenuation time series have been generated for various link characteristics using as input the measured rain rate time series. The SST is used since there are no measurements for

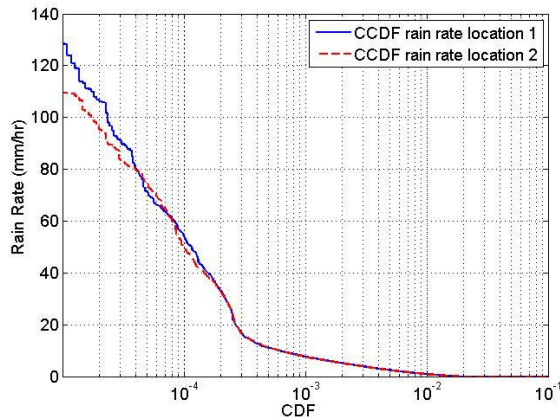


Figure 1. CCDF of rain rate for two years for the two sites.

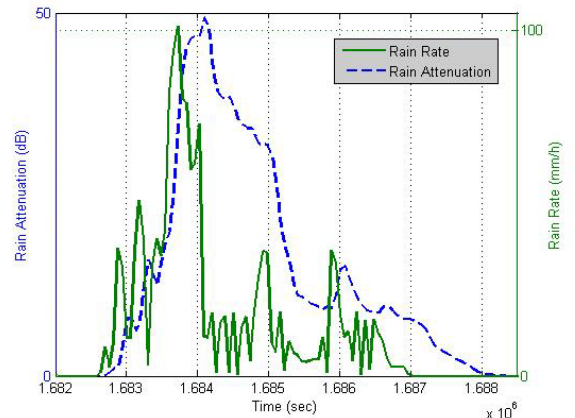


Figure 2. Rain attenuation event and the corresponding rainfall rate event.

Athens. In Fig. 2 an example of rain attenuation time series for a rain event is shown. The corresponding rainfall rate event is also depicted. The SST has been applied to the rain rate measurements for an elevation angle of 30°, frequency of 20 GHz and wind speed equal to 5 m/s. However, the models based on SDEs do not necessitate the measurement of rain rate time series, thus making it easier to be used. According to the model presented in [3], the spectrum of the underline Gaussian process of rain attenuation stochastic process is:

$$PSD(f) = 1 / \left[1 + \left(\frac{2\pi f}{\beta_A} \right)^2 \right] \tag{1}$$

where β_A is the dynamic parameter of rain attenuation. As can be observed, the dynamics of rain attenuation depend on the parameter β_A .

In this paper, the two methods are used in a complementary manner in order to be able to synthesize rain attenuation data for various link characteristics and proceed to the modeling of the dynamic parameter β_A . It must be noted that for the SST, the analysis on the dynamics and power spectrum of rain attenuation modeled with SST has been presented in [16]. It must be noted that rain attenuation power spectrum is modeled in a different way with SST than the SDE based model (Eq. (1)). However, it has been observed in [6] that SST can be used for the extraction of the dynamic parameter through the fitting of the PSD of synthesized data to the theoretical expression (Eq. (1)) with good accuracy. The values obtained in [6] and in this work are comparable to those obtained by other studies (see [6]). Therefore, the SST here is used in order to be able to synthesize rain attenuation data for a great number of link characteristics and used in order to parameterize a SDE based synthesizer which takes a smaller number of parameters as input than SST.

For the same configuration as in Fig. 2, but with wind speed equal to 7 m/s the power spectral density of the underlined Gaussian process of rain attenuation is given in Fig. 3. In the same figure the theoretical PSD of 1 is depicted after its fitting to the experimental PSD. For this specific example the dynamic parameter is equal to $1.25 \cdot 10^{-2} \text{ min}^{-1}$. Here it must be noted that the dynamic parameter of rain rate derived from the experimental time series is $9.12 \cdot 10^{-2} \text{ min}^{-1}$ a value higher than this of rain attenuation, as this is expected [3].

3. UNIFIED RAIN ATTENUATION SYNTHESIZER

As reported in the introduction section, dynamic parameter depends on the link characteristics and climatic region. Therefore, in order to obtain a synthesizer which is able to reproduce time series of rain attenuation for satellite links with different characteristics, an expression is needed for the dynamic parameter. The climatic characteristics determine the dynamic parameter of rainfall rate.

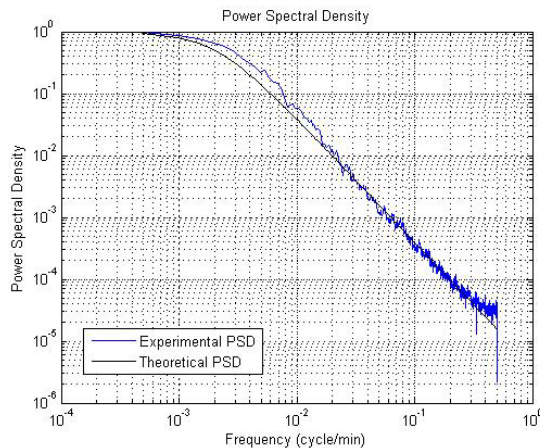


Figure 3. Experimental and fitted PSD of rain attenuation.

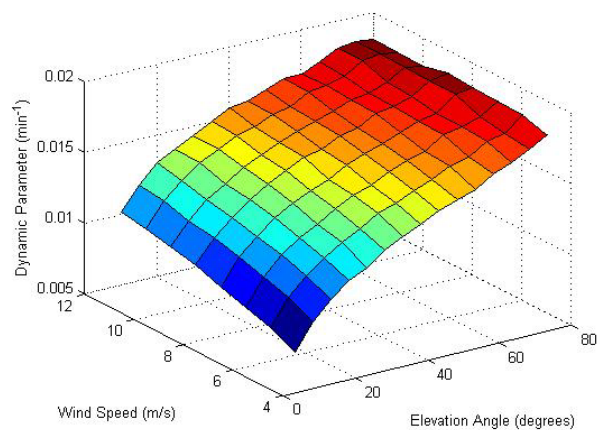


Figure 4. 3D plot of dynamic parameter as a function of wind speed and elevation angle.

An extensive investigation of the sensitivity of the dynamic parameters to the various parameters of the link has been presented in [6]. It was found that the dynamic parameter of rain attenuation mostly depends on wind speed and elevation angle. Therefore, the proposed model will be an expression of these two parameters and the dynamic parameter of rain rate. As explained in the previous section we first applied the SST to the rain rate measurements for typical values of the wind speed from 5 m/sec to 12 m/sec with a step of 1 m/sec and for elevation angle from 10° to 80° with step of 5° . In Fig. 4, the obtained values of the dynamic parameters for these cases are shown.

It can be observed that with the increase of elevation angle and wind speed the dynamic parameter is increased. This occurs due to the decrease of autocorrelation of the rainfall medium for the latter case and due to the increase of path length for the former case.

From fitting procedures, the following expression is found:

$$\beta_A = \beta_R (0.0053V + 0.002) \theta^{-0.0228V + 0.5285} \quad (2)$$

where V is the wind speed (m/sec), θ the elevation angle in degrees, β_R the dynamic parameter of rain rate.

Consequently, based on the previous expression a unified rain attenuation time series synthesizer is presented in Fig. 5. Using as input, the first order statistical parameters of lognormal distribution of rain rate (R_m , S_R), the dynamic parameter of rain rate (β_R) and the link characteristics (elevation angle θ , frequency f and polarization angle τ), the statistical parameters of rain attenuation (A_m , S_A) can be calculated through the methodology presented in [5] and also employing (2), the dynamic parameter of rain attenuation is computed. Then using the analytical solution of Langevin SDE given in [4], the time series of process X_t are generated and through the transform $A(t) = A_m \exp(S_A X_t)$ the rain attenuation time series are obtained. Here we employ the proposed synthesizer for the derivation of rain attenuation series for two different values of elevation angle. The time series snapshots are shown in Fig. 6, for two links with Ground station located at Athens, operating frequency at 30 GHz and 45° and 20° elevation angle. For the computation of the dynamic parameter of rain attenuation, the wind speed was considered equal to 12 m/s. As shown in Fig. 6, the decrease of elevation angle has a high impact on the time series, increasing the rate of change.

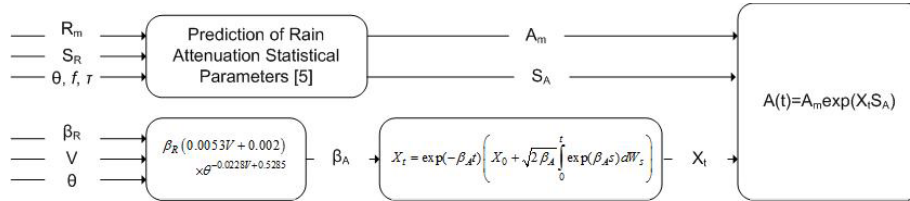


Figure 5. Block diagram of the unified rain attenuation time series synthesizer.

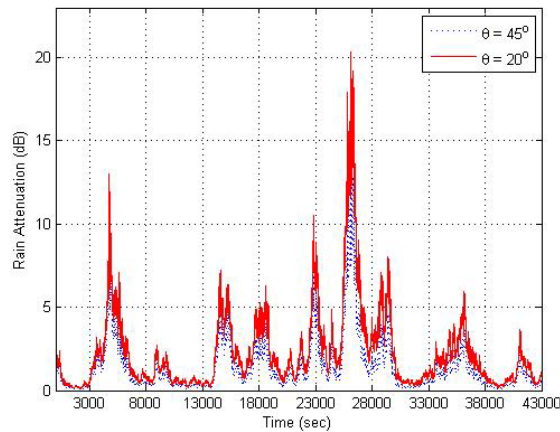


Figure 6. Time series of rain attenuation synthesized with the unified rain attenuation synthesizer model for two different links.

4. DYNAMIC DIVERSITY GAIN

In site diversity systems the satellite communicates with more than one Earth-stations. In this kind of configuration, the probability that rain attenuation takes a value above a certain threshold is lower than the case of a single Earth-satellite link. Therefore, a gain is observed in comparison to single satellite links. This gain is called diversity gain and it is calculated as:

$$DG = A_{SL} - A_{SD} \tag{3}$$

where A_{SL} is the rain attenuation induced on a single link, used as a reference and A_{SD} , rain attenuation induced on the system.

In case that the site diversity satellite system with n ground stations also adopts the Selection Combining (SC), the rain attenuation induced on the system is:

$$A_{SC} = \min\{A_1, A_2, \dots, A_n\} \tag{4}$$

where A_i , with $i = 1, \dots, n$, is the rain attenuation induced in all links. In classical approaches, including the recommendation of ITU-R. P. 618 [17], the diversity gain is computed from 3, for a given time percentage, i.e., the values of attenuation exceed for a P% over a year. However, the diversity gain has also been defined as the dynamic diversity gain using the following notation [9]:

$$G_D(t) = A_S(t) - A_J(t) \tag{5}$$

In the above equation, the diversity gain is defined on temporal domain rather than on time percentage as in [18, 19]. The variable $A_J(t)$ is:

$$A_J(t) = \min \{A_1(t), A_2(t), \dots, A_n(t)\} \tag{6}$$

Using the rain rate data as described previously and applying the SST, we obtain rain attenuation time series for the two sites. The availability of joint rainfall rate time series is 100%. Using (5), the diversity gain can be calculated. In Fig. 7, a snapshot of diversity gain is shown for a dual site diversity system with wind speed equal to 10 m/s, elevation angle 30° and operating frequency 20 GHz. It can be observed that a gain exists even for this small separation distance, i.e., 387 m. For the same configuration, the exceedance probability of diversity gain is given, in Fig. 2. A diversity gain of more than 10 dB for time percentage lower than 0.01% can be achieved, showing that pico-scale diversity systems can be very effective for rain attenuation mitigation. Here, it must be noted that the significance of pico-scale diversity systems has been highlighted in [10]. In the analysis of the later paper, a diversity gain (considering the expression for a certain exceedance percentage of attenuation) of 6–8 dB for high attenuation values (low probability levels) has been found.

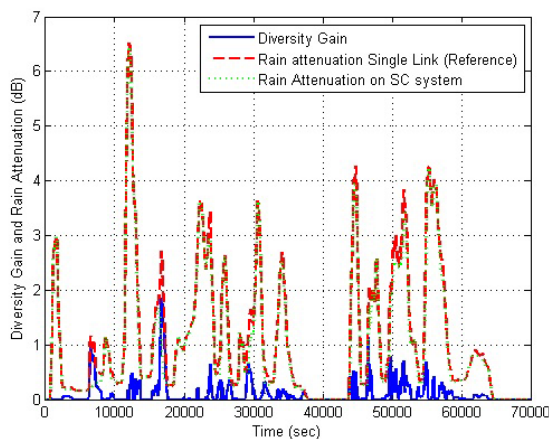


Figure 7. Time series of dynamic diversity gain, joint rain attenuation and rain attenuation induced on the single link used as reference.

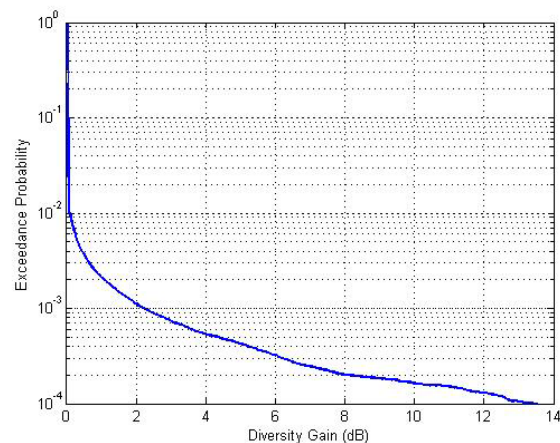


Figure 8. CCDF of dynamic diversity gain.

5. NUMERICAL RESULTS AND DISCUSSION

In this section, firstly, the expression given in (2) is compared to the actual values of the dynamic parameter of rain attenuation for the calculation of the relative error and then a unified a rain attenuation synthesizer is presented. The data set by which (2) is derived is used. As aforementioned, the dynamic parameter of rain rate for this particular case is $9.12 \cdot 10^{-2} \text{ min}^{-1}$. The error for this first data set is shown in Table 1. The RMS error is small and equal to 3.1%. However, such small value is expected since this data set has been already used for the derivation of the tested expression. Therefore, a second data set is used in which rain rate time series measured at the campus of NTUA for the same time period but at a different spatial point than this of the first data set are used for the derivation of the dynamic parameter of rain attenuation as explained in the previous sections. The dynamic parameter of rain rate at the second data set is $9.31 \cdot 10^{-2} \text{ min}^{-1}$. Now, using the theoretical expression of 2, the error is computed for this second data set and shown in Table 1. It can be observed that for this case too the error remains low and equal to 5.61%.

In the same table the statistics of the error are shown for the same two data sets, but for a greater frequency of 30 GHz. The error is exactly the same. This may be because as found in [6], the frequency does not play a role on the dynamic parameter of rain attenuation. This may hold since (1) refers to the underlined Gaussian process. However, the similarity on the values of the dynamic parameter on the frequency does not mean that the dynamics of rain attenuation are the same and independent of the frequency, since as shown in [3], the temporal correlation of rain attenuation depends also on the mean value and standard deviation of rain attenuation.

Considering the dynamic diversity gain, it has been shown in Fig. 8 that a diversity gain can be observed for a pico-scale site diversity system. Here, using the synthesized data, the CCDF of the dynamic diversity gain is calculated for a link of 20 GHz and 30° elevation angle for two different values of wind speed: 7 m/s and 12 m/s. The results are shown in Fig. 9. It can be observed that the gain

Table 1. Mean value, standard deviation and RMS value of the relative error in % for two different data sets and for frequency equal to 20 GHz and 30 GHz.

Data Set — freq (GHz)	ϵ_{mean}	ϵ_{std}	ϵ_{RMS}
1–20	0.3	3.1	3.1
2–20	4.7	3	5.6
1–30	0.3	3.1	3.1
2–30	4.7	3	5.6

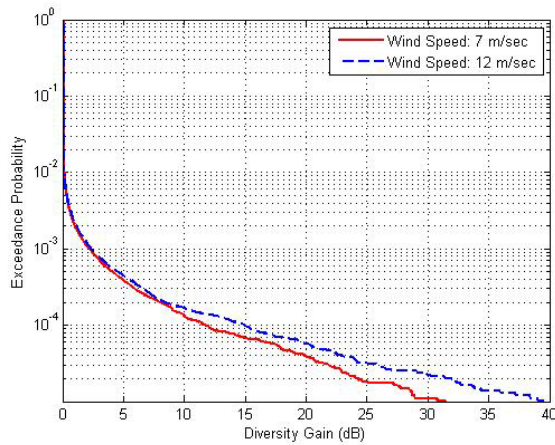


Figure 9. CCDF of diversity gain for wind speed: 7 m/s, 12 m/s.

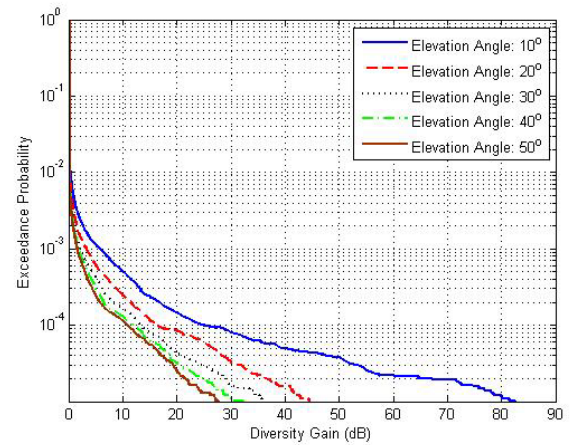


Figure 10. CCDF of diversity gain for various elevation angles.

is increased when the wind speed is increased. Moreover, the CCDF has been calculated for different elevation angles. The results are shown in Fig. 10. Here it is observed that the dynamic diversity gain is higher for low elevation angles. All these curves can be used for the efficient evaluation and installation of broadband pico-scale site diversity systems operating at Ku band and above.

6. CONCLUSION

In this paper, firstly, an expression for the calculation of the dynamic parameter of rain attenuation is presented. The expression is given as a function of the wind speed, elevation angle and dynamic parameter of rain rate. Then a unified rain attenuation synthesizer is proposed based on SDEs, which takes into account the various characteristics (climatic and link) for the generation of rain attenuation time series. It can be used for the calculation of the first (long term exceedance probability) and second order statistics (fade slope, fade durations, autocorrelation and hitting time statistics) of slant path rain attenuation with various electrical and geometrical characteristics. Moreover, the proposed model can be applied to the prediction of the performance of satellite fade mitigation techniques, such as Time diversity [20], or adaptive coding and modulation and power control. Also, with the extension of the model to multidimensional case [21], the proposed model can be used for interference analysis evaluation [22] and for the prediction of the fade margins for broadband wireless access networks [23]. Finally, the dynamic diversity gain is evaluated for a pico-scale site diversity system. The dynamic diversity gain in general can be used for the design of pico-scale site diversity systems, such a sports event broadcast with the antennas established around the stadium and also for smart diversity systems.

REFERENCES

1. Panagopoulos, A. D., P.-D. Arapoglou, and P. G. Cottis, "Satellite communications at Ku, Ka and V bands: Propagation impairments and mitigation techniques," *IEEE Communication Surveys and Tutorials*, Vol. 6, No. 3, 2–14, 2004.
2. Morello, A. and U. Reimers, "DVB-S2, the second generation standard for satellite broadcasting and unicasting," *International Journal of Satellite Communications and Networking*, Vol. 22, 249–268, 2004.
3. Maseng, T. and P. Bakken, "A stochastic dynamic model of rain attenuation," *IEEE Transactions on Communications*, Vol. 29, No. 5, 660–669, 1981.
4. Kanellopoulos, S. A., A. D. Panagopoulos, and J. D. Kanellopoulos, "Calculation of the dynamic input parameter for a stochastic model simulating rain attenuation: A novel mathematical approach," *IEEE Transactions on Antennas and Propagation*, Vol. 55, No. 11, Part 2, 3257–3264, 2007.
5. Panagopoulos, A. D. and J. D. Kanellopoulos, "On the rain attenuation dynamics: Spatial-temporal analysis of rainfall-rate and fade duration statistics," *International Journal of Satellite Communications and Networking*, Vol. 21, No. 6, 595–611, 2003.
6. Kourogorgas, C. I., A. D. Panagopoulos, J. D. Kanellopoulos, S. N. Livieratos, and G. E. Chatzarakis, "Investigation of rain fade dynamic properties using simulated rain attenuation data with synthetic storm technique," *2013 7th European Conference on Antennas and Propagation (EuCAP)*, 2277–2281, Apr. 8–12, 2013.
7. Andrade, F. J. A. and L. A. R. da Silva Mello, "Rain attenuation time series synthesize based on the gamma distribution," *IEEE Antennas and Wireless Propag. Letters*, Vol. 10, 1381–1384, 2011.
8. Cheffena, M., L. E. Braten, and T. Ekman, "On the space-time variations of rain attenuation," *IEEE Transactions on Antennas and Propagation*, Vol. 57, No. 6, 1771–1782, 2009.
9. Enjamio, C., E. Vilar, D. Ndzi, and F. Perez Fontan, "Short-scale diversity in a dynamic rain fade environment," *International Journal of Satellite Communications and Networking*, Vol. 23, 143–152, 2005.
10. Matricciani, E., "Micro scale site diversity in satellite and tropospheric communication systems affected by rain attenuation," *Space Communications*, Vol. 19, 83–90, IOS Press, 2003.

11. Matricciani, E., "Physical-mathematical model of the dynamics of rain attenuation based on rain rate time series and a two-layer vertical structure of precipitation," *Radio Science*, Vol. 31, No. 2, 281–295, 1996.
12. Karlin, S. and H. Taylor, *A Second Course in Stochastic Processes*, Academic, New York, 1981.
13. Karatzas, I. and S. E. Shreve, *Brownian Motion and Stochastic Calculus*, Springer-Verlag, NY, 1991.
14. Matricciani, E. and C. Riva, "The search for the most reliable long-term rain attenuation CDF of a slant path and the impact on propagation models," *IEEE Transactions on Antennas and Propagation*, Vol. 53, No. 7, 2307–2313, 2005.
15. Kourogiorgas, C., A. D. Panagopoulos, et al., "Analysis of 15-months rain rate measurements at NTUA campus," *6th European Conference on Antennas and Propagation*, 505–509, Prague, Czech Republic, Mar. 26–30, 2012.
16. Matricciani, E., "Physical-mathematical model of dynamics of rain attenuation with application to power spectrum," *Electronics Letters*, Vol. 30, No. 6, 522–524, Mar. 17, 1994.
17. ITU-R. P. 618-10, "Propagation data and prediction methods required for the design of Earth-space communication systems," Geneva, 2009.
18. Hodge, D. B., "An improved model for diversity gain on Earth-space propagation paths," *Radio Science*, Vol. 17, No. 6, 1393–1399, 1982.
19. Luini, L. and C. Capsoni, "A rain cell model for the simulation and performance evaluation of site diversity schemes," *IEEE Antennas and Wireless Propag. Letters*, Vol. 12, 1327–1330, 2013.
20. Kourogiorgas, C., A. D. Panagopoulos, S. N. Livieratos, and G. E. Chatzarakis, "On the outage probability prediction of time diversity scheme in broadband satellite communication systems," *Progress In Electromagnetics Research C*, Vol. 44, 175–184, 2013.
21. Karagiannis, G. A., A. D. Panagopoulos, and J. D. Kanellopoulos, "Multidimensional rain attenuation stochastic dynamic modeling: Application to Earth-space diversity systems," *IEEE Transactions on Antennas and Propagation*, Vol. 60, No. 11, 5400–5411, 2012.
22. Kanellopoulos, J. D., A. D. Panagopoulos, and S. N. Livieratos, "Differential rain attenuation statistics including an accurate estimation of the effective slant path lengths," *Journal of Electromagnetic Waves and Applications*, Vol. 14, No. 5, 663–664, 2000; *Progress In Electromagnetics Research*, Vol. 28, 97–120, 2000.
23. Rafi Ul Islam, M., T. A. Rahman, S. K. B. A. Rahim, K. F. Al-Tabatabaie, and A. Y. Abdulrahman, "Fade margins prediction for broadband fixed wireless access (BFWA) from measurements in tropics," *Progress In Electromagnetics Research C*, Vol. 11, 199–212, 2009.